Rapid transmission and tight bottlenecks constrain the evolution of highly transmissible SARS-CoV-2 variants

Emily E. Bendall[1], Amy Callear[2], Amy Getz[2], Kendra Goforth[2], Drew Edwards[2], Arnold S. Monto[2], Emily T. Martin[2], Adam S. Lauring[1,3 *]

[1]Department of Microbiology and Immunology, University of Michigan, Ann Arbor, MI, USA

[2]Department of Epidemiology, University of Michigan, Ann Arbor, MI, USA

[3]Division of Infectious Diseases, Department of Internal Medicine, University of Michigan, Ann Arbor, MI, USA

*** Corresponding Author**:

Adam Lauring

MS2 4742C, SPC 1621

1137 Catherine Street, Ann Arbor, MI 48109

alauring@med.umich.edu.

Keywords: SARS-CoV-2; transmission; bottleneck; genomic epidemiology

Running Title: SARS-CoV-2 diversity in households

Abstract Word Count: 240

Main Text Word Count: 3410

Abstract

Transmission bottlenecks limit the spread of novel mutations and reduce the efficiency of natural selection along a transmission chain. Many viruses exhibit tight bottlenecks, and studies of early SARS-CoV-2 lineages identified a bottleneck of 1-3 infectious virions. While increased force of infection, host receptor binding, or immune evasion may influence bottleneck size, the relationship between transmissibility and the transmission bottleneck is unclear. Here, we compare the transmission bottleneck of non-variant-of-concern (non-VOC) SARS-CoV-2 lineages to those of the Alpha, Delta, and Omicron variants. We sequenced viruses from 168 individuals in 65 multiply infected households in duplicate to high depth of coverage. In 110 specimens collected close to the time of transmission, within-host diversity was extremely low. At a 2% frequency threshold, 51% had no intrahost single nucleotide variants (iSNV), and 42% had 1-2 iSNV. In 64 possible transmission pairs with detectable iSNV, we identified a bottleneck of 1 infectious virion (95% CI 1-1) for Alpha, Delta, and Omicron lineages and 2 (95% CI 2-2) in non-VOC lineages. The latter was driven by a single iSNV shared in one non-VOC household. The tight transmission bottleneck in SARS-CoV-2 is due to low genetic diversity at the time of transmission, a relationship that may be more pronounced in rapidly transmissible variants. The tight bottlenecks identified here will limit the development of highly mutated VOC in typical transmission chains, adding to the evidence that selection over prolonged infections in immunocompromised patients may drive their evolution.

Introduction

Viral populations are often subject to multiple bottleneck events as they evolve within and between hosts. These bottlenecks drastically reduce the size and genetic diversity of the population, which will affect how new mutations spread through host populations (1, 2). In the setting of a tight transmission bottleneck, most mutations that arise within a host are not propagated between them. Bottlenecks also reduce the virus's effective population size, which captures the number of virions that reproduce and genetically contribute to the next generation; selection is less effective in smaller populations. Therefore, tight bottlenecks constrain adaptive evolution by limiting the spread of newly arising mutations and reducing the efficiency of selection on these mutations along transmission chains. Many viruses, such as HIV (3, 4), influenza (5), and SARS-CoV-2 (6–10), have tight bottlenecks, with 1-3 distinct viral genomes transmitted.

The size of the transmission bottleneck may be impacted by viral dynamics, route of infection, or molecular interactions at the virus-host interface. For example, it has been suggested that transmissibility, or force of infection, may influence bottleneck size. Increased transmissibility may lead to wider bottlenecks in several ways. First, increasing the infectious dose, perhaps through increased shedding in the donor host or increased intensity of contact, can lead to wider bottlenecks as shown in experimental infections of influenza A virus (11, 12) and tobacco etch virus (13). Additionally, the number of virions that initially infect cells is directly related to bottleneck size (14). More transmissible viruses may have an increased ability to infect

42 individual cells, such as through increased receptor affinity or escape from intrinsic or innate
43 immunity.
44
45 While early studies of SARS-CoV-2 transmission estimated a tight transmission bottleneck, the
46 last 20 months of the pandemic have witnessed the emergence of highly transmissible variants
47 of concern (VOC). In December 2020, B.1.1.7 (Alpha) was detected for the first time with a
48 substantial increase in transmissibility over previous SARs-CoV-2 lineages (15). Since then,
49 additional variants of concern characterized by an increase in transmissibility have arisen. The
50 Alpha, Beta, Gamma, Delta, and Omicron VOC are 25-100% more transmissible than the original
51 Wuhan strain (16). There are multiple and overlapping mechanisms for the increased
52 transmissibility in SARS-CoV-2 that may influence bottleneck size, including increased binding to
53 ACE2 (17–20), increased viral shedding (21, 22), innate immune evasion (23), rapid cellular
54 penetration (18), and alternative entry pathways (24, 25).
55
56 Here we explore the relationship between viral transmissibility and transmission bottlenecks by
57 comparing bottleneck size across multiple VOC and pre-VOC lineages. We sampled viral
58 populations from two household cohorts in Michigan, obtaining high depth of coverage
59 sequence from 168 individuals in 65 households. We found that bottleneck size did not vary
60 significantly between transmission pairs infected with pre-VOC lineages and those infected with
61 highly transmissible Alpha, Delta, or Omicron (BA.1) lineages. This tight bottleneck was largely
62 the result of limited diversity in the donor host at the time of transmission.
63

Methods

Households and sample collection

Households were enrolled through two household cohorts in Southeast Michigan – MHome and the Household Influenza Vaccine Evaluation Study (HIVE). MHome is a case ascertained household cohort in which households are recruited following identification of an index case who meets a case definition for COVID-like illness and is positive for SARS-CoV-2 by clinical testing. Households in this study were enrolled between November 18, 2020 and January 19, 2022. HIVE is a prospective household cohort with year-round surveillance for symptomatic acute respiratory illness. We identified all HIVE households with ≥1 individuals positive for SARS-CoV-2 between June 1, 2021 and January 18, 2022. For both studies, written informed consent (paper or electronic) was obtained from adults (aged >18). Parents or legal guardians of minor children provided written informed consent on behalf of their children. Both study protocols were reviewed and approved by the University of Michigan Institutional Review Board (HIVE: HUM118900 & HUM198212, MHome: HUM180896).

In MHome, index enrollees meeting the case definition (at least one the following: cough, difficulty breathing, or shortness of breath; or at least two of the following: fever, chills, rigors, myalgia, headache, sore throat, new loss of smell or taste) with a positive clinical test result within the last 7 days are invited to enroll themselves and their household members. Nasal swabs were collected on days 0, 5, and 10 after enrollment for all participating household members. For HIVE, study participants were instructed to collect a nasal swab at the onset of illness, with weekly active confirmation of illness status by study staff. Eligible illness was

defined as two or more of cough, nasal congestion, sore throat, chills, fever/feverish, body aches, or headache (for participants 3 years & older) or two or more of cough, runny nose/nasal congestion, fever/feverish, fussiness/irritability, decreased appetite, trouble breathing, or fatigue (for participants under 3 years old). If a participant had symptoms of a respiratory illness, specimens were collected from all members of that household on days 0, 5, and 10 of the index illness. For both cohorts all samples were nasal swabs that were self-collected, or in the case of young children, parent-collected following an established protocol (26). In both cohorts, participants were questioned about the day of symptom onset and duration of symptoms. In MHome, the index case was defined as the individual with the earliest symptom onset date. If two or more individuals shared the earliest onset date, they were considered to be co-index cases.

Viral sequencing

All samples were tested by quantitative reverse transcriptase polymerase chain reaction (RT-qPCR) with either the TaqPath COVID-19 Combo Kit from Thermofisher (MHome) or CDC Influenza SARS-CoV-2 Multiplex Assay (HIVE). We sequenced the first positive sample in each individual with a cycle threshold (Ct) value ≤30 from each individual. RNA was extracted using the MagMAX viral/pathogen nucleic acid purification kit (ThermoFisher) and a KingFisher Flex instrument. Sequencing libraries were prepared using the NEBNext ARTIC SARS-CoV-2 Library Prep Kit (NEB) and ARTIC V3 (MHome, through November 10, 2021) and V4 (MHome, after November 10, 2021; HIVE) primer sets. After barcoding, libraries were pooled in equal volume. The pooled libraries (up to 96 samples per pool) were size selected by gel extraction and

sequenced on an illumina MiSeq (2x250, v2 chemistry). We sequenced all samples in duplicate from the RNA extraction step onwards, randomizing sample position on the plate between replicates.

We aligned the sequencing reads to the MN908947.3 reference using BWA-mem v 0.7.15 (27). Primers were trimmed and consensus sequences were generated using iVar v1.2.1 (28). Intrahost single nucleotide variants (iSNV) were identified for each replicate separately using iVar (28) with the following criteria: average genome wide coverage >500x, frequency 0.02-0.98, p-value $<1x10^{-5}$, variant position coverage depth > 400x. We also masked ambiguous and homoplastic sites (29). Finally, to minimize the possibility of false variants being detected, the variants had to be present in both sequencing replicates. Indels were not evaluated.

Delineation of transmission chains and SARS-CoV-2 lineages

Alignments of consensus sequences within each household were manually inspected. We considered infections to be consistent with household transmission if the consensus sequences differed by ≤2 mutations (30). We excluded individuals whose consensus sequences were inconsistent with household transmission but retained the rest of the household if there was evidence of household transmission among the other members. Households were split and analyzed separately if the consensus sequences supported multiple independent transmission chains within the household. If necessary, we reassigned the index case, so that the index case was part of the transmission chain.

For households with genetically linked infections, we further analyzed all samples with high quality sequencing (>500x coverage) from households with ≥2 members. We used Nextclade to annotate clades and variants of concern (31). We used the WHO definition to classify variants of concern (i.e., Alpha, Beta, Gamma, Delta, and Omicron: BA1)(32). Variants of interest were included in the non-variants of concern group for all analyses.

Infection dynamics

Serial intervals were calculated as the time between symptom onset of the index and each household contact and compared across clades using an ANOVA. Additionally, the times between symptom onset and sample collection for index cases were calculated. Serial intervals and time to sampling across clades were compared using an ANOVA followed by a Tukey HSD. We also compared the Ct values from the nucleocapsid gene of sequenced samples and the other positive non-sequenced samples for index cases.

Bottleneck estimation

We defined the possible transmission pairs within each household as follows: the index was allowed to be the donor for household contacts, and the household contacts were allowed to be donors to each other. The only case in which the index case was allowed to be the recipient was when there were co-index cases. Co-index cases were allowed to be both donor and recipient with respect to the other co-index. After defining the transmission pairs, we applied the approximate beta-binomial approach (33). This method accounts for the variant calling frequency threshold and stochasticity in the recipient after transmission. We estimated the

bottleneck size for each transmission pair individually and also calculated an overall bottleneck size for each clade using a weighted sum of loglikelihoods (33). We re-calculated the above bottleneck estimates after merging replicate aligned fastq files to examine the impact of our variant calling strategy.

Data and materials availability

Raw sequencing reads are available on the NCBI short read archive under BioProject PRJNA889424 . Data and scripts necessary to replicate the analyses are available on github (https://github.com/lauringlab/SARS-CoV-2_VOC_transmission_bottleneck).

Results

We used high depth of coverage sequencing to characterize SARS-CoV-2 populations collected from individuals enrolled in a prospective surveillance cohort (HIVE) and a case-ascertained household cohort (MHome). There were 65 multiply infected households (infections ≤14 days apart) with 168 cases. High quality, whole genome sequences (see Methods) were obtained with technical replicates from 131 cases. Depth of coverage was generally high and iSNV frequency was similar across both replicates (Figure S1). There were five households that had consensus sequences inconsistent with household transmission (Figure S2). Of these five, two households with two individuals each were excluded. In two households, there was a single individual whose consensus sequence differed from the others and was excluded. In the final household, the consensus sequences were consistent with two separate transmission pairs, and these were analyzed separately. All 5 households with multiple introductions were due to

174 either Delta or Omicron viruses, consistent with high community prevalence during these
175 waves (34). The final transmission analysis dataset included 45 households, 110 individuals, and
176 134 possible transmission pairs (Table 1). Alpha (B.1.1.7), Gamma (P.1), Delta (AY.3, AY.4,
177 AY.39, AY.44, AY.100), and Omicron (BA.1, BA.1.1) were represented in these households.
178 Variants of interest included one household with Lambda (C.37).
179
180 There was rapid transmission of SARS-CoV-2 in the sampled households. The median serial
181 interval ranged between 2 and 3.5 with no significant difference observed between clades (df
182 =4, F =.879, p =0.483, Figure 1A, Figure S3). Households with Delta and Omicron had a greater
183 range of serial intervals. Viral specimens were collected soon after symptom onset in both
184 household studies, with a clade-specific medians ranging from 2-6.5 days. Omicron had a
185 shorter time between index symptom onset and sample collection for sequencing than non-
186 VOC (df=3, F=8.138, p <0.001) and Alpha (p =0.01) (Figure 1B, S3). This is likely due to the
187 number of Omicron cases in HIVE households, which had a shorter time between index
188 symptom onset and sample collection for sequencing than MHome households (df =1, F
189 =15.363, p < 0.001).
190
191 We further examined the timing of index case sampling by trending RT-qPCR Ct values for all
192 index case specimens. In nearly all cases, the index cases were sampled at peak viral shedding
193 (Figure 1C). Therefore, our sequence data for the index cases should be reflective of the genetic
194 diversity present in donor hosts when risk of household transmission was highest. Consistent
195 with the short time between the infection onset and sample collection, we found low genetic

196 diversity in nearly all specimens. (Figure 2A). A majority (56/110, 51%) had no iSNV above the
197 2% frequency threshold; 42% (46/110) of samples had 1-2 iSNV; and 7% (8/110) had $\geq$ 3 iSNV.
198 There were no specimens with more than 5 iSNV. Fifty-two percent of iSNV were present at
199 <10% frequency within hosts, Figure 2B).
200
201 Bottleneck size is calculated based on shared diversity between members of a transmission
202 pair. Within each household, possible transmission pairs included the index case as donor and
203 each household contact as a recipient, and household contacts as donors for other household
204 contact recipients. While the majority of sampled households had only two cases, 12 had three
205 cases, and 4 had four cases (Figure 3A). The number of possible transmission pairs per
206 household ranged from 1 to 12 (Table S1). When we compared the frequency of iSNV in the
207 donors and recipients, we found only a single shared iSNV – C29708T (noncoding) – in 6
208 possible transmission pairs from a single household (Figure 3B). This iSNV was present in all
209 three individuals in the household at a frequency of 0.56, 0.97, and 0.24 respectively. All other
210 iSNV were either absent (frequency of 0) or completely fixed (frequency of 1) in the other
211 individual of the transmission pair for all households. This pattern is highly suggestive of a
212 narrow bottleneck.
213
214 We used the beta binomial model (33) to obtain a quantitative estimate of the transmission
215 bottleneck. Because bottleneck size can only be calculated when there are iSNV in the
216 transmission donor (see Figure 2A), we were able to use 64 potential pairs in this analysis (Table
217 S1). All VOC clades had an overall bottleneck size of 1 (Alpha, Delta, Omicron: 95% CI 1:1,

Gamma: 95% CI 1:7). The Non-VOC clades had an overall bottleneck size of 2 (95% CI 2:2), which was driven entirely by the single shared iSNV in one household. The 6 transmission pairs in this household exhibited bottlenecks of 2, 4, and 6 (Table S2). All other transmission pairs had a bottleneck size of 1 inclusive of all clades. Across all transmission pairs, the upper bound of the 95% confidence interval varied greatly, from 1 to 200, the maximum bottleneck size we evaluated (Table S2).

We were stringent in our variant calling criteria and required iSNV to be present in both sequencing replicates, because false positive iSNV can artifactually inflate bottleneck estimates (7, 35–37). To ensure that our stringency did not lead to an underestimate, we re-analyzed our dataset after merging sequencing reads across the technical replicates. This had only a small effect on the number of iSNV identified in each specimen (Figure S4). Thirty-nine out of 110 specimens still had no iSNV present, and all but 2 specimens had ≤8 iSNV. The remaining two specimens had 25 and 57 iSNV. The newly detected iSNV in the merged dataset tended to be present at very low frequency (<3%) and shifted the iSNV frequency distribution toward lower values (Figure S4). In this lower stringency dataset, an additional 19 transmission pairs had iSNV in the donor. However, the bottleneck sizes for all clades were identical to the previous estimates (Table S3). This suggests that the tight bottlenecks we estimated were not due to overly stringent variant calling.

Discussion

Here, we used in depth sequencing of two well-sampled household cohorts to define the relationship between transmissibility and transmission bottleneck size. We found that all clades exhibited short serial intervals in our households and low genetic diversity in specimens collected close to the time of transmission. This limited genetic diversity across all clades resulted in a tight estimated bottleneck. In line with bottleneck estimates for first-wave lineages of SARS-CoV-2 we found that VOC clades had a bottleneck of 1 and non-VOC had a bottleneck of 2. These very tight bottleneck estimates were robust to reductions in the stringency in variant-calling.

Consistent with prior studies of SARS-CoV-2 and other viruses, we found low genetic diversity within and between hosts. Allowing for slight differences due to analytic pipelines, previous studies have largely reported low within-host genetic diversity in SARS-CoV-2 (6, 9, 38–40). Much of this diversity is not shared between hosts, as multiple studies in different settings have measured a tight transmission bottleneck for SARS-CoV-2 (6–10). Tight bottlenecks appear to be broadly applicable across routes of infection and viral family. Potato Y virus (0.5-3.2) and Cucumber mosaic virus (1-2), both transmitted by aphids (41, 42), along with Influenza (1-2), HIV (3, 4), Venezuelan equine encephalitis (43), and HCV (44) have tight bottlenecks .

Additionally, we demonstrate that increased transmissibility, whether through force of infection or immune escape, doesn't change the bottleneck size for SARS-CoV-2. Genetic diversity constrains bottleneck sizes, and with sufficiently low genetic diversity the bottleneck cannot be greater than one. For both non-VOC and VOC, the short generation time of SARS-

CoV-2 does not allow for diversity to accumulate in the donor, much less transmit. These effects may be exaggerated in highly transmissible variants if time to transmission is shortened. While we did not find variant-specific differences in serial interval in our cohorts, multiple studies that explicitly modeled generation time during household transmission have shown shorter generation times as the pandemic has progressed. Even before variants of concern arose, the generation time of SARS-CoV-2 was decreasing (45), and this trend continued as variants of concern arose with Delta (3.2 days) exhibiting a shorter generation time than Alpha (4.5 days) (46). A shortening of generation could potentially have a larger impact on bottleneck size for other viruses, particularly those that generate more diversity than SARS-CoV-2 prior to transmission.

Our work highlights how transmission bottlenecks, as typically measured, are distinct from infectious dose. Within-host processes in the recipient influence bottleneck size, because not all virions that initiate an infection go on to establish a genetic lineage (1). After infection begins, stochastic loss (genetic drift) during exponential growth, superinfection exclusion, cell-to-cell heterogeneity, and host immune response cause some virions to be lost (47). These within-host processes combined with the starting genetic diversity cause bottleneck size to, in many cases, be smaller than the infectious dose. In experimental systems, genetic barcoding and more frequent sampling of donor and recipient hosts can be used to link bottlenecks to infectious dose and identify lineages that are lost (12, 48).

Our study is subject to at least three limitations. First, in all studies of natural transmission, there is always some ambiguity about who infected whom. In two-infection households, it is possible that both were exposed to a common donor outside the household, and in households with >2 cases, there are multiple possible transfection pairs. Because individuals who don't transmit to each other are unlikely to share diversity, incorrect pairing will underestimate the bottleneck (5). However, we found that all transmission pairs had equal bottlenecks even when we tested mutually exclusive transmission pairs. Second, virus populations may be spatially segregated within hosts, and the transmitted population may not have been well sampled by our analysis of nasal swabs (49–53). However, given the low viral diversity identified in nearly all cases, even spatially segregated viral populations are likely to be genetically similar to each other. Third, rare diversity may have been under sampled in the donors and recipients due to the sensitivity of our sequencing approach. This possibility was addressed in our analysis of merged technical replicates. Given that more common variants (10-50% frequency) were not shared between hosts, it is unlikely that even perfect detection would find shared iSNV at lower frequencies.

Understanding how different viral properties promote or impede evolution is critical for predicting and effectively monitoring the course of the COVID pandemic. The tight bottlenecks we have estimated for SARS-CoV-2 VOC will both limit the spread of new mutations and reduce the effectiveness of natural selection. Weakened selection will inhibit the evolution of new lineages and may be especially important for new VOC. Whereas other lineages may evolve through non-selective mechanisms, such as genetic drift, the existing VOC have exhibited

304 strong signals of prior positive selection at the time of their emergence (16)(54–56). The tight
305 bottlenecks identified here will limit the development of highly mutated VOC in typical
306 transmission chains, adding to the evidence that selection over prolonged infections in
307 immunocompromised patients may drive the evolution of SARS-CoV-2 variants of concern (6,
308 15, 57, 58).
309
310 **Acknowledgements**
311 We thank all individuals who participated in this study. This project has been funded in in part
312 with Federal funds from the National Institute of Allergy and Infectious Diseases, National
313 Institutes of Health, Department of Health and Human Services, under Contract No.
314 75N93021C00015 and R01 AI148371 and from the Centers for Disease Control and Prevention,
315 under U01IP001034.
316

References

1. Zwart MP, Elena SF. 2015. Matters of Size: Genetic Bottlenecks in Virus Infection and Their Potential Impact on Evolution. Annu Rev Virol 2:161–79.

2. McCrone JT, Lauring AS. 2018. Genetic bottlenecks in intraspecies virus transmission. Curr Opin Virol 28:20–25.

3. Edwards CT, Holmes EC, Wilson DJ, Viscidi RP, Abrams EJ, Phillips RE, Drummond AJ. 2006. Population genetic estimation of the loss of genetic diversity during horizontal transmission of HIV-1. BMC Evol Biol 6:28.

4. Keele BF, Giorgi EE, Salazar-Gonzalez JF, Decker JM, Pham KT, Salazar MG, Sun C, Grayson T, Wang S, Li H, Wei X, Jiang C, Kirchherr JL, Gao F, Anderson JA, Ping L-H, Swanstrom R, Tomaras GD, Blattner WA, Goepfert PA, Kilby JM, Saag MS, Delwart EL, Busch MP, Cohen MS, Montefiori DC, Haynes BF, Gaschen B, Athreya GS, Lee HY, Wood N, Seoighe C, Perelson AS, Bhattacharya T, Korber BT, Hahn BH, Shaw GM. 2008. Identification and characterization of transmitted and early founder virus envelopes in primary HIV-1 infection. Proc Natl Acad Sci 105:7552–7557.

5. McCrone JT, Woods RJ, Martin ET, Malosh RE, Monto AS, Lauring AS. 2018. Stochastic processes constrain the within and between host evolution of influenza virus. eLife 7:e35962.

6. Braun K, Moreno G, Wagner C, Accola MA, Rehrauer WM, Baker D, Koelle K, O'Connor DH, Bedford T, Friedrich TC, Moncla LH. 2021. Limited within-host diversity and tight

337 transmission bottlenecks limit SARS-CoV-2 evolution in acutely infected individuals.
338 bioRxiv https://doi.org/10.1101/2021.04.30.440988.

339 7. Martin MA, Koelle K. 2021. Comment on “Genomic epidemiology of superspreading
340 events in Austria reveals mutational dynamics and transmission properties of SARS-CoV-
341 2.” Sci Transl Med 13.

342 8. Nicholson MD, Endler L, Popa A, Genger J-W, Bock C, Michor F, Bergthaler A. 2021.
343 Response to comment on “Genomic epidemiology of superspreading events in Austria
344 reveals mutational dynamics and transmission properties of SARS-CoV-2.” Sci Transl Med
345 13:eabj3222.

346 9. Hannon WW, Roychoudhury P, Xie H, Shrestha L, Addetia A, Jerome KR, Greninger AL,
347 Bloom JD. 2022. Narrow transmission bottlenecks and limited within-host viral diversity
348 during a SARS-CoV-2 outbreak on a fishing boat. Virus Evol 8:1–9.

349 10. Li B, Deng A, Li K, Hu Y, Li Z, Shi Y, Xiong Q, Liu Z, Guo Q, Zou L, Zhang H, Zhang M,
350 Ouyang F, Su J, Su W, Xu J, Lin H, Sun J, Peng J, Jiang H, Zhou P, Hu T, Luo M, Zhang
351 Y, Zheng H, Xiao J, Liu T, Tan M, Che R, Zeng H, Zheng Z, Huang Y, Yu J, Yi L, Wu J,
352 Chen J, Zhong H, Deng X, Kang M, Pybus OG, Hall M, Lythgoe KA, Li Y, Yuan J, He J,
353 Lu J. 2022. Viral infection and transmission in a large, well-traced outbreak caused by the
354 SARS-CoV-2 Delta variant. Nat Commun 13:460.

355 11. Tao H, Steel J, Lowen AC. 2014. Intrahost Dynamics of Influenza Virus Reassortment. J
356 Virol 88:7485–7492.

12. Varble A, Albrecht RA, Backes S, Crumiller M, Bouvier NM, Sachs D, García-Sastre A, tenOever BR. 2014. Influenza A Virus Transmission Bottlenecks Are Defined by Infection Route and Recipient Host. Cell Host Microbe 16:691–700.

13. Zwart MP, Daròs J-A, Elena SF. 2011. One Is Enough: In Vivo Effective Population Size Is Dose-Dependent for a Plant RNA Virus. PLOS Pathog 7:e1002122.

14. Koelle K, Lin J, Zhu H, Antia R, Lowen AC, Weissman D. 2022. Masks Do No More Than Prevent Transmission: Theory and Data Undermine the Variolation Hypothesis. medRxiv https://doi.org/10.1101/2022.06.28.22277028.

15. Hill V, Du Plessis L, Peacock TP, Aggarwal D, Colquhoun R, Carabelli AM, Ellaby N, Gallagher E, Groves N, Jackson B, McCrone JT, O'Toole Á, Price A, Sanderson T, Scher E, Southgate J, Volz E, Barclay WS, Barrett JC, Chand M, Connor T, Goodfellow I, Gupta RK, Harrison EM, Loman N, Myers R, Robertson DL, Pybus OG, Rambaut A, The COVID-19 genomics UK (COG-UK) consortium. 2022. The Origins and Molecular Evolution of SARS-CoV-2 Lineage B.1.1.7 in the UK. Virus Evol veac080.

16. Telenti A, Hodcroft EB, Robertson DL. 2022. The Evolution and Biology of SARS-CoV-2 Variants. Cold Spring Harb Perspect Med 12:1–24.

17. Cai Y, Zhang1 J, Xiao T, Lavine CL, Rawson S, Peng H, Zhu7 H, Anand K, Tong P, Gautam A, Lu S, Sterling SM, Walsh Jr. RM, Rits-Volloch S, Lu J, Wesemann DR, Yang W, Seaman MS, Chen B. 2021. Structural basis for enhanced infectivity and immune evasion of SARS-CoV-2 variants. Science 373:642–648.

18. Zhang J, Xiao T, Cai Y, Lavine CL, Peng H, Zhu H, Anand K, Tong P, Gautam A, Mayer ML, Walsh RM, Rits-Volloch S, Wesemann DR, Yang W, Seaman MS, Lu J, Chen B. 2021. Membrane fusion and immune evasion by the spike protein of SARS-CoV-2 Delta variant. Science 374:1353–1360.

19. Araf Y, Akter F, Tang Y, Fatemi R, Parvez MdSA, Zheng C, Hossain MdG. 2022. Omicron variant of SARS-CoV-2: Genomics, transmissibility, and responses to current COVID-19 vaccines. J Med Virol 94:1825–1832.

20. Kumar S, Thambiraja TS, Karuppanan K, Subramaniam G. 2022. Omicron and Delta variant of SARS-CoV-2: A comparative computational study of spike protein. J Med Virol 94:1641–1649.

21. Syed AM, Taha TY, Khalid MM, Tabata T, Chen IP, Sreekumar B, Chen P-Y, Hayashi JM, Soczek KM, Ott M, Doudna JA. 2021. Rapid assessment of SARS-CoV-2–evolved variants using virus-like particles. Science 374:1626–1632.

22. Puhach O, Adea K, Hulo N, Sattonnet P, Genecand C, Iten A, Jacquérioz F, Kaiser L, Vetter P, Eckerle I, Meyer B. 2022. Infectious viral load in unvaccinated and vaccinated individuals infected with ancestral, Delta or Omicron SARS-CoV-2. Nat Med 28:1491–1500.

23. Thorne LG, Bouhaddou M, Reuschl A-K, Zuliani-Alvarez L, Polacco B, Pelin A, Batra J, Whelan MVX, Hosmillo M, Fossati A, Ragazzini R, Jungreis I, Ummadi M, Rojc A, Turner J, Bischof ML, Obernier K, Braberg H, Soucheray M, Richards A, Chen K-H, Harjai B, Memon D, Hiatt J, Rosales R, McGovern BL, Jahun A, Fabius JM, White K,

Goodfellow IG, Takeuchi Y, Bonfanti P, Shokat K, Jura N, Verba K, Noursadeghi M, Beltrao P, Kellis M, Swaney DL, García-Sastre A, Jolly C, Towers GJ, Krogan NJ. 2022. Evolution of enhanced innate immune evasion by SARS-CoV-2. 7897. Nature 602:487–495.

24. Hui KPY, Ho JCW, Cheung M, Ng K, Ching RHH, Lai K, Kam TT, Gu H, Sit K-Y, Hsin MKY, Au TWK, Poon LLM, Peiris M, Nicholls JM, Chan MCW. 2022. SARS-CoV-2 Omicron variant replication in human bronchus and lung ex vivo. 7902. Nature 603:715–720.

25. Meng B, Abdullahi A, Ferreira IATM, Goonawardane N, Saito A, Kimura I, Yamasoba D, Gerber PP, Fatihi S, Rathore S, Zepeda SK, Papa G, Kemp SA, Ikeda T, Toyoda M, Tan TS, Kuramochi J, Mitsunaga S, Ueno T, Shirakawa K, Takaori-Kondo A, Brevini T, Mallery DL, Charles OJ, The CITIID-NIHR BioResource COVID-19 Collaboration, Baker S, Dougan G, Hess C, Kingston N, Lehner PJ, Lyons PA, Matheson NJ, Ouwehand WH, Saunders C, Summers C, Thaventhiran JED, Toshner M, Weekes MP, Maxwell P, Shaw A, Bucke A, Calder J, Canna L, Domingo J, Elmer A, Fuller S, Harris J, Hewitt S, Kennet J, Jose S, Kourampa J, Meadows A, O'Brien C, Price J, Publico C, Rastall R, Ribeiro C, Rowlands J, Ruffolo V, Tordesillas H, Bullman B, Dunmore BJ, Gräf S, Hodgson J, Huang C, Hunter K, Jones E, Legchenko E, Matara C, Martin J, Mescia F, O'Donnell C, Pointon L, Shih J, Sutcliffe R, Tilly T, Treacy C, Tong Z, Wood J, Wylot M, Betancourt A, Bower G, Cossetti C, De Sa A, Epping M, Fawke S, Gleadall N, Grenfell R, Hinch A, Jackson S, Jarvis I, Krishna B, Nice F, Omarjee O, Perera M, Potts M, Richoz N, Romashova V, Stefanucci L, Strezlecki M, Turner L, De Bie EMDD, Bunclark K, Josipovic M, Mackay M, Butcher H, Caputo D, Chandler M, Chinnery P, Clapham-Riley D, Dewhurst E,

421 Fernandez C, Furlong A, Graves B, Gray J, Hein S, Ivers T, Le Gresley E, Linger R,
422 Kasanicki M, King R, Kingston N, Meloy S, Moulton A, Muldoon F, Ovington N, Papadia
423 S, Penkett CJ, Phelan I, Ranganath V, Paraschiv R, Sage A, Sambrook J, Scholtes I, Schon
424 K, Stark H, Stirrups KE, Townsend P, Walker N, Webster J, The Genotype to Phenotype
425 Japan (G2P-Japan) Consortium, Butlertanaka EP, Tanaka YL, Ito J, Uriu K, Kosugi Y,
426 Suganami M, Oide A, Yokoyama M, Chiba M, Motozono C, Nasser H, Shimizu R,
427 Kitazato K, Hasebe H, Irie T, Nakagawa S, Wu J, Takahashi M, Fukuhara T, Shimizu K,
428 Tsushima K, Kubo H, Kazuma Y, Nomura R, Horisawa Y, Nagata K, Kawai Y, Yanagida
429 Y, Tashiro Y, Tokunaga K, Ozono S, Kawabata R, Morizako N, Sadamasu K, Asakura H,
430 Nagashima M, Yoshimura K, Ecuador-COVID19 Consortium, Cárdenas P, Muñoz E,
431 Barragan V, Márquez S, Prado-Vivar B, Becerra-Wong M, Caravajal M, Trueba G, Rojas-
432 Silva P, Grunauer M, Gutierrez B, Guadalupe JJ, Fernández-Cadena JC, Andrade-Molina
433 D, Baldeon M, Pinos A, Bowen JE, Joshi A, Walls AC, Jackson L, Martin D, Smith KGC,
434 Bradley J, Briggs JAG, Choi J, Madissoon E, Meyer KB, Mlcochova P, Ceron-Gutierrez L,
435 Doffinger R, Teichmann SA, Fisher AJ, Pizzuto MS, de Marco A, Corti D, Hosmillo M,
436 Lee JH, James LC, Thukral L, Veesler D, Sigal A, Sampaziotis F, Goodfellow IG,
437 Matheson NJ, Sato K, Gupta RK. 2022. Altered TMPRSS2 usage by SARS-CoV-2
438 Omicron impacts infectivity and fusogenicity. Nature 603:706–714.

439 26. Malosh RE, Petrie JG, Callear AP, Monto AS, Martin ET. 2021. Home collection of nasal
440 swabs for detection of influenza in the Household Influenza Vaccine Evaluation Study.
441 Influenza Other Respir Viruses 15:227–234.

442 27. Li H, Durbin R. 2009. Fast and accurate short read alignment with Burrows-Wheeler
443 transform. Bioinformatics 25:1754–1760.

444 28. Grubaugh ND, Gangavarapu K, Quick J, Matteson NL, De Jesus JG, Main BJ, Tan AL,
445 Paul LM, Brackney DE, Grewal S, Gurfield N, Van Rompay KKA, Isern S, Michael SF,
446 Coffey LL, Loman NJ, Andersen KG. 2019. An amplicon-based sequencing framework for
447 accurately measuring intrahost virus diversity using PrimalSeq and iVar. Genome Biol
448 20:8.

449 29. De Maio N, Walker C, Borges R, Weilguny L, Slodkowicz G, Goldman Ni. 2020. Issues
450 with SARS-CoV-2 sequencing data. Virological.

451 30. Bendall E, Paz-Bailey G, Santiago GA, Porucznik CA, Stanford JB, Stockwell MS, Duque
452 J, Jeddy Z, Veguilla V, Major C, Rivera-Amill V, Rolfes MA, Dawood FS, Lauring AS.
453 2022. SARS-CoV-2 genomic diversity in households highlights the challenges of sequence-
454 based transmission inference. medRxiv https://doi.org/10.1101/2022.08.09.22278452.

455 31. Aksamentov I, Roemer C, Hodcroft EB, Neher RA. 2021. Nextclade: clade assignment,
456 mutation calling and quality control for viral genomes. J Open Source Softw 6:3773.

457 32. 2022. Tracking SARS-CoV-2 variants. https://www.who.int/activities/tracking-SARS-
458 CoV-2-variants. Retrieved 29 August 2022.

459 33. Sobel Leonard A, Weissman DB, Greenbaum B, Ghedin E, Koelle K. 2017. Transmission
460 Bottleneck Size Estimation from Pathogen Deep-Sequencing Data, with an Application to
461 Human Influenza A Virus. J Virol 91:e00171-17.

462 34. Petrie JG, Eisenberg MC, Lauring AS, Gilbert J, Harrison SM, DeJonge PM, Martin ET.
463 2022. The variant-specific burden of SARS-CoV-2 in Michigan: March 2020 through
464 November 2021. J Med Virol 94:5251–5259.

35. Poon LLM, Song T, Rosenfeld R, Lin X, Rogers MB, Zhou B, Sebra R, Halpin RA, Guan Y, Twaddle A, DePasse JV, Stockwell TB, Wentworth DE, Holmes EC, Greenbaum B, Peiris JSM, Cowling BJ, Ghedin E. 2016. Quantifying influenza virus diversity and transmission in humans. 2. Nat Genet 48:195–200.

36. Xue KS, Bloom JD. 2019. Reconciling disparate estimates of viral genetic diversity during human influenza infections. 9. Nat Genet 51:1298–1301.

37. Popa A, Genger J-W, Nicholson MD, Penz T, Schmid D, Aberle SW, Agerer B, Lercher A, Endler L, Colaço H, Smyth M, Schuster M, Grau ML, Martínez-Jiménez F, Pich O, Borena W, Pawelka E, Keszei Z, Senekowitsch M, Laine J, Aberle JH, Redlberger-Fritz M, Karolyi M, Zoufaly A, Maritschnik S, Borkovec M, Hufnagl P, Nairz M, Weiss G, Wolfinger MT, von Laer D, Superti-Furga G, Lopez-Bigas N, Puchhammer-Stöckl E, Allerberger F, Michor F, Bock C, Bergthaler A. 2020. Genomic epidemiology of superspreading events in Austria reveals mutational dynamics and transmission properties of SARS-CoV-2. Sci Transl Med 12:eabe2555.

38. Lythgoe KA, Hall M, Ferretti L, de Cesare M, MacIntyre-Cockett G, Trebes A, Andersson M, Otecko N, Wise EL, Moore N, Lynch J, Kidd S, Cortes N, Mori M, Williams R, Vernet G, Justice A, Green A, Nicholls SM, Ansari MA, Abeler-Dörner L, Moore CE, Peto TEA, Eyre DW, Shaw R, Simmonds P, Buck D, Todd JA, on behalf of the Oxford Virus Sequencing Analysis Group (OVSG), Connor TR, Ashraf S, da Silva Filipe A, Shepherd J, Thomson EC, The COVID-19 Genomics UK (COG-UK) Consortium, Bonsall D, Fraser C, Golubchik T. 2021. SARS-CoV-2 within-host diversity and transmission. Science 372:eabg0821.

487 39. Tonkin-Hill G, Martincorena I, Amato R, Lawson AR, Gerstung M, Johnston I, Jackson
488 DK, Park N, Lensing SV, Quail MA, Gonçalves S, Ariani C, Spencer Chapman M,
489 Hamilton WL, Meredith LW, Hall G, Jahun AS, Chaudhry Y, Hosmillo M, Pinckert ML,
490 Georgana I, Yakovleva A, Caller LG, Caddy SL, Feltwell T, Khokhar FA, Houldcroft CJ,
491 Curran MD, Parmar S, The COVID-19 Genomics UK (COG-UK) Consortium, Alderton A,
492 Nelson R, Harrison EM, Sillitoe J, Bentley SD, Barrett JC, Torok ME, Goodfellow IG,
493 Langford C, Kwiatkowski D, Wellcome Sanger Institute COVID-19 Surveillance Team.
494 2021. Patterns of within-host genetic diversity in SARS-CoV-2. eLife 10:e66857.

495 40. Valesano AL, Rumfelt KE, Dimcheff DE, Blair CN, Fitzsimmons WJ, Petrie JG, Martin
496 ET, Lauring AS. 2021. Temporal dynamics of SARS-CoV-2 mutation accumulation within
497 and across infected hosts. PLOS Pathog 17:e1009499.

498 41. Ali A, Li H, Schneider WL, Sherman DJ, Gray S, Smith D, Roossinck MJ. 2006. Analysis
499 of Genetic Bottlenecks during Horizontal Transmission of Cucumber Mosaic Virus. J Virol
500 80:8345–8350.

501 42. Moury B, Fabre F, Senoussi R. 2007. Estimation of the number of virus particles
502 transmitted by an insect vector. Proc Natl Acad Sci 104:17891–17896.

503 43. Smith DR, Adams AP, Kenney JL, Wang E, Weaver SC. 2008. Venezuelan equine
504 encephalitis virus in the mosquito vector Aedes taeniorhynchus: infection initiated by a
505 small number of susceptible epithelial cells and a population bottleneck. Virology 372:176–
506 186.

507 44. Bull RA, Luciani F, McElroy K, Gaudieri S, Pham ST, Chopra A, Cameron B, Maher L,
508 Dore GJ, White PA, Lloyd AR. 2011. Sequential Bottlenecks Drive Viral Evolution in
509 Early Acute Hepatitis C Virus Infection. PLoS Pathog 7:e1002243.

510 45. Hart WS, Abbott S, Endo A, Hellewell J, Miller E, Andrews N, Maini PK, Funk S,
511 Thompson RN. 2022. Inference of the SARS-CoV-2 generation time using UK household
512 data. eLife 11:e70767.

513 46. Hart WS, Miller E, Andrews NJ, Waight P, Maini PK, Funk S, Thompson RN. 2022.
514 Generation time of the alpha and delta SARS-CoV-2 variants: an epidemiological analysis.
515 Lancet Infect Dis 22:603–610.

516 47. Gutiérrez S´n, Michalakis Y, Blanc Ś phane. 2012. Virus population bottlenecks during
517 within-host progression and host-to-host transmission. Curr Opin Virol 2.

518 48. Weger-Lucarelli J, Garcia SM, Rückert C, Byas A, O'Connor SL, Aliota MT, Friedrich TC,
519 O'Connor DH, Ebel GD. 2018. Using barcoded Zika virus to assess virus population
520 structure in vitro and in Aedes aegypti mosquitoes. Virology 521:138–148.

521 49. Hamada N, Hara K, Kashiwagi T, Imamura Y, Nakazono Y, Watanabe H, Imamura Y,
522 Chijiwa K. 2012. Intrahost emergent dynamics of oseltamivir-resistant virus of pandemic
523 influenza A (H1N1) 2009 in a fatally immunocompromised patient. J Infect Chemother
524 18:865–871.

525 50. Gallagher ME, Brooke CB, Ke R, Koelle K. 2018. Causes and Consequences of Spatial
526 Within-Host Viral Spread. 11. Viruses 10:627.

527 51. Desai N, Neyaz A, Szabolcs A, Shih AR, Chen JH, Thapar V, Nieman LT, Solovyov A,
528 Mehta A, Lieb DJ, Kulkarni AS, Jaicks C, Xu KH, Raabe MJ, Pinto CJ, Juric D, Chebib I,
529 Colvin RB, Kim AY, Monroe R, Warren SE, Danaher P, Reeves JW, Gong J, Rueckert EH,
530 Greenbaum BD, Hacohen N, Lagana SM, Rivera MN, Sholl LM, Stone JR, Ting DT,
531 Deshpande V. 2020. Temporal and spatial heterogeneity of host response to SARS-CoV-2
532 pulmonary infection. 1. Nat Commun 11:6319.

533 52. Ganti K, Bagga A, Ferreri LM, Geiger G, Carnaccini S, Caceres CJ, Seibert B, Li Y, Wang
534 L, Kwon T, Li Y, Morozov I, Ma W, Richt JA, Perez DR, Koelle K, Lowen AC. 2022.
535 Influenza A virus reassortment in mammals gives rise to genetically distinct within-host
536 sub-populations. bioRxiv https://doi.org/10.1101/2022.02.08.479600.

537 53. Farjo M, Koelle K, Martin MA, Gibson LL, Walden KKO, Rendon G, Fields CJ, Alnaji
538 FG, Gallagher N, Luo CH, Mostafa HH, Manabe YC, Pekosz A, Smith RL, McManus DD,
539 Brooke CB. 2022. Within-host evolutionary dynamics and tissue compartmentalization
540 during acute SARS-CoV-2 infection. bioRxiv https://doi.org/10.1101/2022.06.21.497047.

541 54. van Dorp L, Richard D, Tan CCS, Shaw LP, Acman M, Balloux F. 2020. No evidence for
542 increased transmissibility from recurrent mutations in SARS-CoV-2. 1. Nat Commun
543 11:5986.

544 55. MacLean OA, Orton R, Singer JB, Robertson DL. 2020. Response to “On the origin and
545 continuing evolution of SARS-CoV-2.”

546 56. Molina-Mora JA, Reales-González J, Camacho E, Duarte-Martínez F, Tsukayama P, Soto-
547 Garita C, Brenes H, Cordero-Laurent E, Santos AR dos, Salgado CG, Silva CS, Souza JS

548 de, Nunes G, Negri T, Vidal A, Oliveira R, Oliveira G, Muñoz-Medina JE, Lais AGS,
549 Mireles-Rivera G, Sosa E, Turjanski A, Monzani MC, Carobene MG, Lenicov FR,
550 Schottlender G, Porto DAFD, Kreuze JF, Sacristán L, Guevara-Suarez M, Cristancho M,
551 Campos-Sánchez R, Herrera-Estrella A. 2022. Overview of the SARS-CoV-2 genotypes
552 circulating in Latin America during 2021. bioRxiv
553 https://doi.org/10.1101/2022.08.19.504579.

554 57. Wilkinson SAJ, Richter A, Casey A, Osman H, Mirza JD, Stockton J, Quick J, Ratcliffe L,
555 Sparks N, Cumley N, Poplawski R, Nicholls SN, Kele B, Harris K, Peacock TP, Loman NJ,
556 The COVID-19 Genomics UK (COG-UK) consortium. 2022. Recurrent SARS-CoV-2
557 mutations in immunodeficient patients. Virus Evol 8:veac050.

558 58. Ghafari M, Liu Q, Dhillon A, Katzourakis A, Weissman DB. 2022. Investigating the
559 evolutionary origins of the first three SARS-CoV-2 variants of concern. Front Virol 2.

560

561

562 **Figure Legends**

563

564 Figure 1. Serial interval and timing of sample collection. (A) Days between index symptom onset
565 and household contact symptom onset for the indicated clades. “Non-VOC” includes all lineages
566 not designated as a WHO variant of concern. No Beta variant transmission pairs were analyzed.
567 (B) Days between symptom onset and collection of the sequenced specimen for the index case.
568 Index cases from MHome are indicated in teal, and index cases from HIVE are indicated in red.
569 Omicron had a shorter time between index symptom onset and sample collection for
570 sequencing than non-VOC (df=3, F=8.138, p <0.001) and Alpha. HIVE households had a shorter
571 time than MHome households (df =1, F =15.363, p < 0.001). (C) RT-qPCR cycle threshold values
572 (inverted y-axis) for all specimens collected from index cases. Sequenced specimens are
573 indicated with filled circles.

574

575 Figure 2. Genetic diversity in sequenced specimens. (A) Histogram of the number of iSNV per
576 specimen. (B) iSNV frequency histogram.

577

578 Figure 3. Diversity across transmission pairs. (A) The number of individuals per household with
579 sequenced specimens. Colors represent the different clades. (B) Shared genetic diversity
580 between transmission pairs. Each point is an iSNV within a transmission pair. Red points
581 indicate mutation C29708T, which was shared in a single household (see text).

582

583 Figure S1. Sequencing coverage and consistency. (A) Boxplot of median (+/- IQR) coverage
584 across the genome in 400bp non-overlapping sliding windows. (B) Frequency of iSNV in each
585 replicate for iSNV that were identified in both replicates.
586
587 Figure S2. Inclusion and exclusion of transmission pairs. (A) Examples of possible transmission
588 pairs in households. In each panel, the index cases are in blue, and the household contacts are
589 in black. The grey arrows indicate transmission pairs, and they point from the donor to the
590 recipient. (B) Consensus genome alignments inconsistent with household transmission. The
591 genomes were visualized using Nextclade. Both Nextclade and Pango lineages are reported.
592 Colored bars are mutations with reference to the Wuhan-Hu-1/2019 (MN908947) strain. Gray
593 partial bars indicate missing data. Asterisks next to household names indicate households that
594 were removed from further analyses. Asterisks next to sample names indicate samples that
595 were removed from further analyses, while the rest of the household was retained. The black
596 cross (†) indicates a household with two separate transmission pairs.
597
598 Figure S3. Timing of symptom onset and specimen collection by household. Each panel shows a
599 household, grouped by the indicated clades. Within each household, blue symbols indicate
600 index case(s) and black symbols indicate household contact(s). Open triangles indicate time of
601 symptom onset and filled triangles indicate specimens that were sequenced. If there is no
602 symptom onset, the case was considered to be asymptomatic.
603

Figure S4. Timing of symptom onset and specimen collection by household. Each panel shows a household, grouped by the indicated clades. Within each household, blue symbols indicate index case(s) and black symbols indicate household contact(s). Open triangles indicate time of symptom onset and filled triangles indicate specimens that were sequenced. If there is no symptom onset, the case was considered to be asymptomatic.

Figure S5. iSNV detected when sequencing replicates are merged. (A) The number of iSNV per specimen. Nearly still had a low number of iSNV. However, merging the reads greatly increased the number of iSNV in two individuals. These iSNV were near the 2% threshold. (B) Most iSNV were found at low frequencies. The frequency distribution shifted toward lower frequencies compared to when iSNV had to be detected in both replicates.

616 **Table 1**

	Non-VOC	Alpha	Gamma	Delta	Omicron	Total
Individuals with successful sequencing	22	21	3	25	40	111
Households with successful sequencing*	11	7	1	12	15	46
Possible transmission pairs	26	34	2	19	55	134
Transmission pairs included in bottleneck analysis**	15	19	1	12	17	64

* Households that have 2 or more individuals with successful sequencing

** Only includes transmission pairs where there are iSNV in the donor

617

618

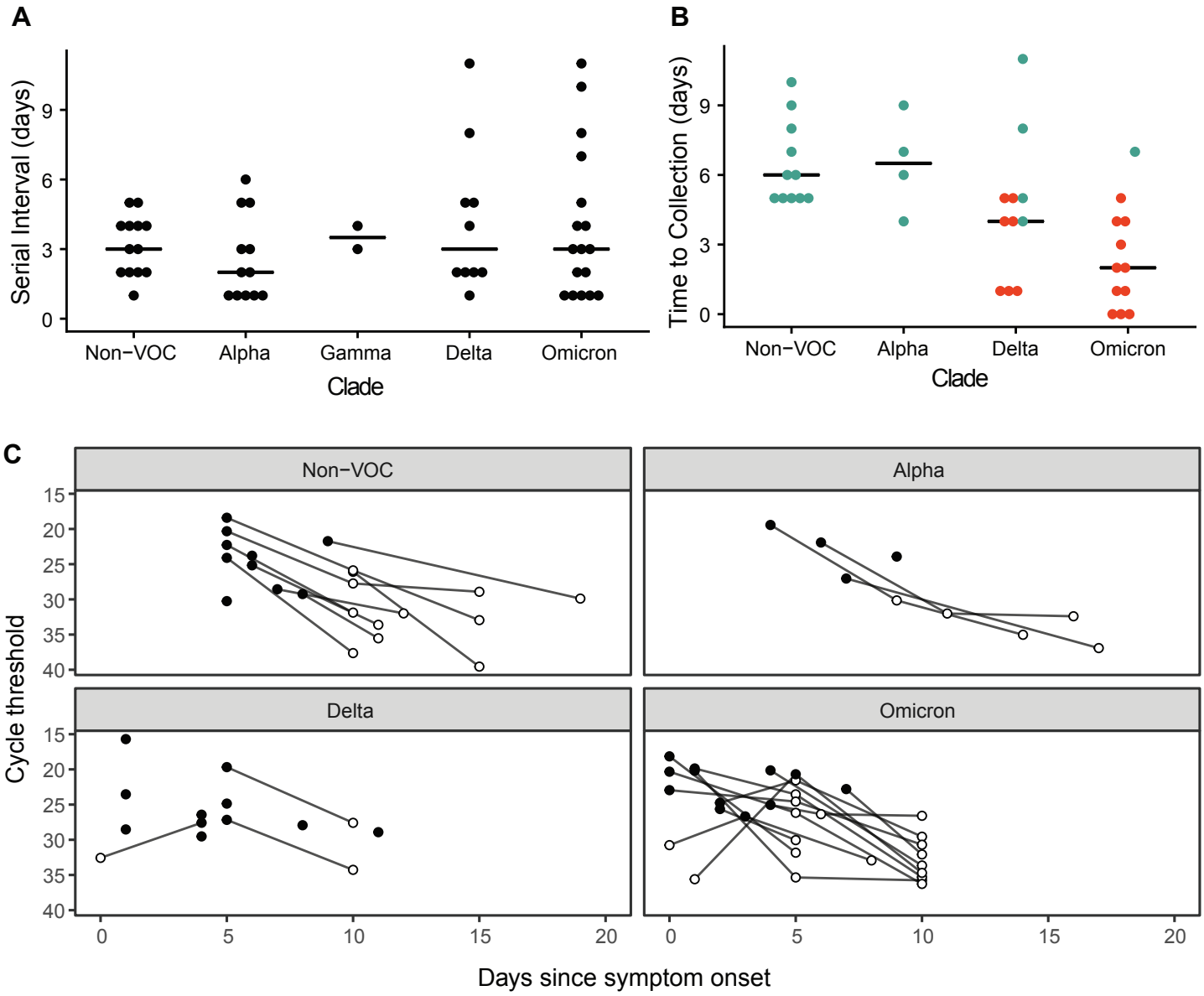

Figure 1. Serial interval and timing of sample collection. (A) Days between index symptom onset and household contact symptom onset for the indicated clades. “Non-VOC” includes all lineages not designated as a WHO variant of concern. No Beta variant transmission pairs were analyzed. (B) Days between symptom onset and collection of the sequenced specimen for the index case. Index cases from MHome are indicated in teal, and index cases from HIVE are indicated in red. Omicron had a shorter time between index symptom onset and sample collection for sequencing than non-VOC (df=3, F=8.138, p <0.001) and HIVE households had a shorter time than MHome households (df =1, F =15.363, p < 0.001). (C) RT-qPCR cycle threshold values (inverted y-axis) for all specimens collected from index cases. Sequenced specimens are indicated with filled circles.

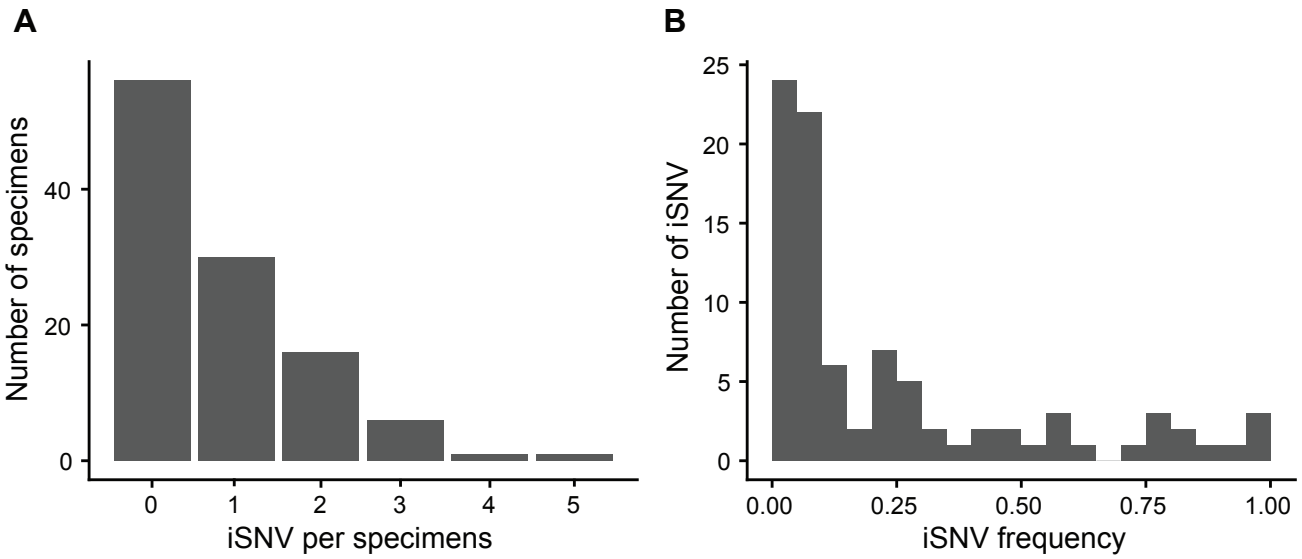

Figure 2. Genetic diversity in sequenced specimens. (A) Histogram of the number of iSNV per specimen. (B) iSNV frequency histogram.

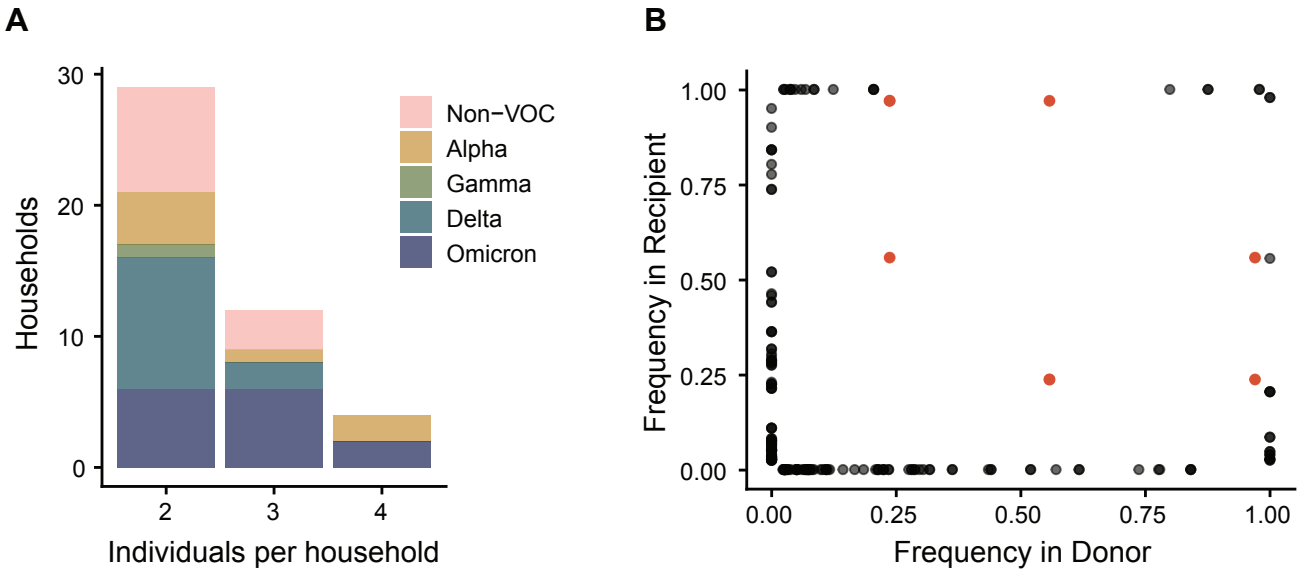

Figure 3. Diversity across transmission pairs. (A) The number of individuals per household with sequenced specimens. Colors represent the different clades. (B) Shared genetic diversity between transmission pairs. Each point is an iSNV within a transmission pair. Red points indicate mutation C29708T, which was shared in a single household.

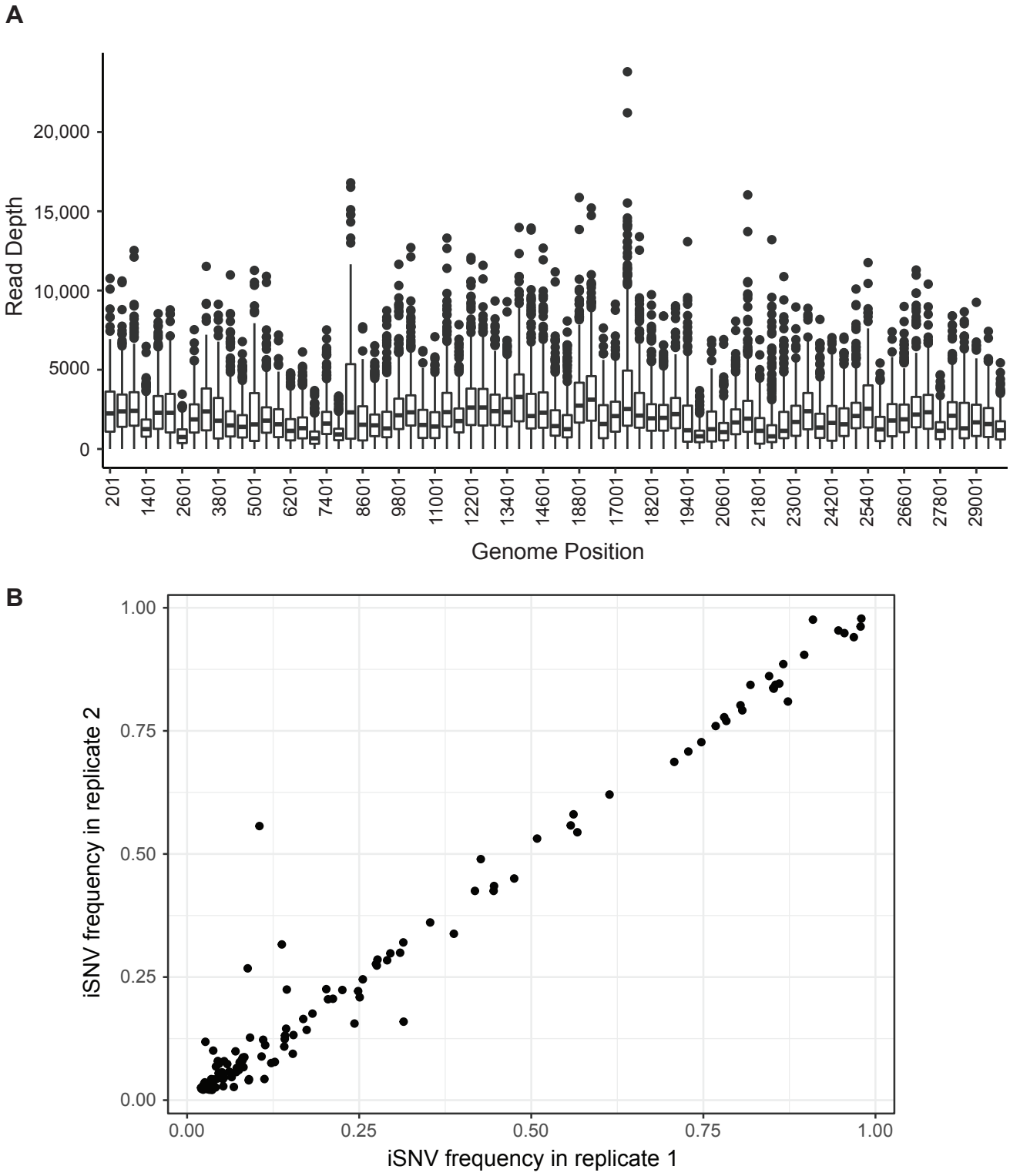

Figure S1. Sequencing coverage and consistency. (A) Boxplot of median (+/- IQR) coverage across the genome in 400bp non-overlapping sliding windows. (B) Frequency of iSNV in each replicate for iSNV that were identified in both replicates.

A

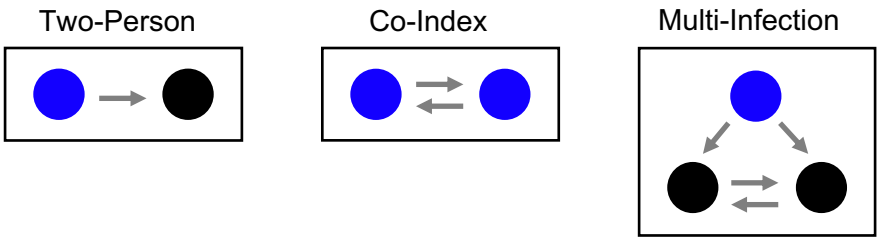

B

Figure S2. Inclusion and exclusion of transmission pairs. (A) Examples of possible transmission pairs in households. In each panel, the index cases are in blue, and the household contacts are in black. The grey arrows indicate transmission pairs, and they point from the donor to the recipient. (B) Consensus genome alignments inconsistent with household transmission. The genomes were visualized using Nextclade. Both Nextclade and Pango lineages are reported. Colored bars are mutations with reference to the Wuhan-Hu-1/2019 (MN908947) strain. Gray partial bars indicate missing data. Asterisks next to household names indicate households that were removed from further analyses. Asterisks next to sample names indicate samples that were removed from further analyses, while the rest of the household was retained. The black cross (†) indicates a household with two separate transmission pairs.

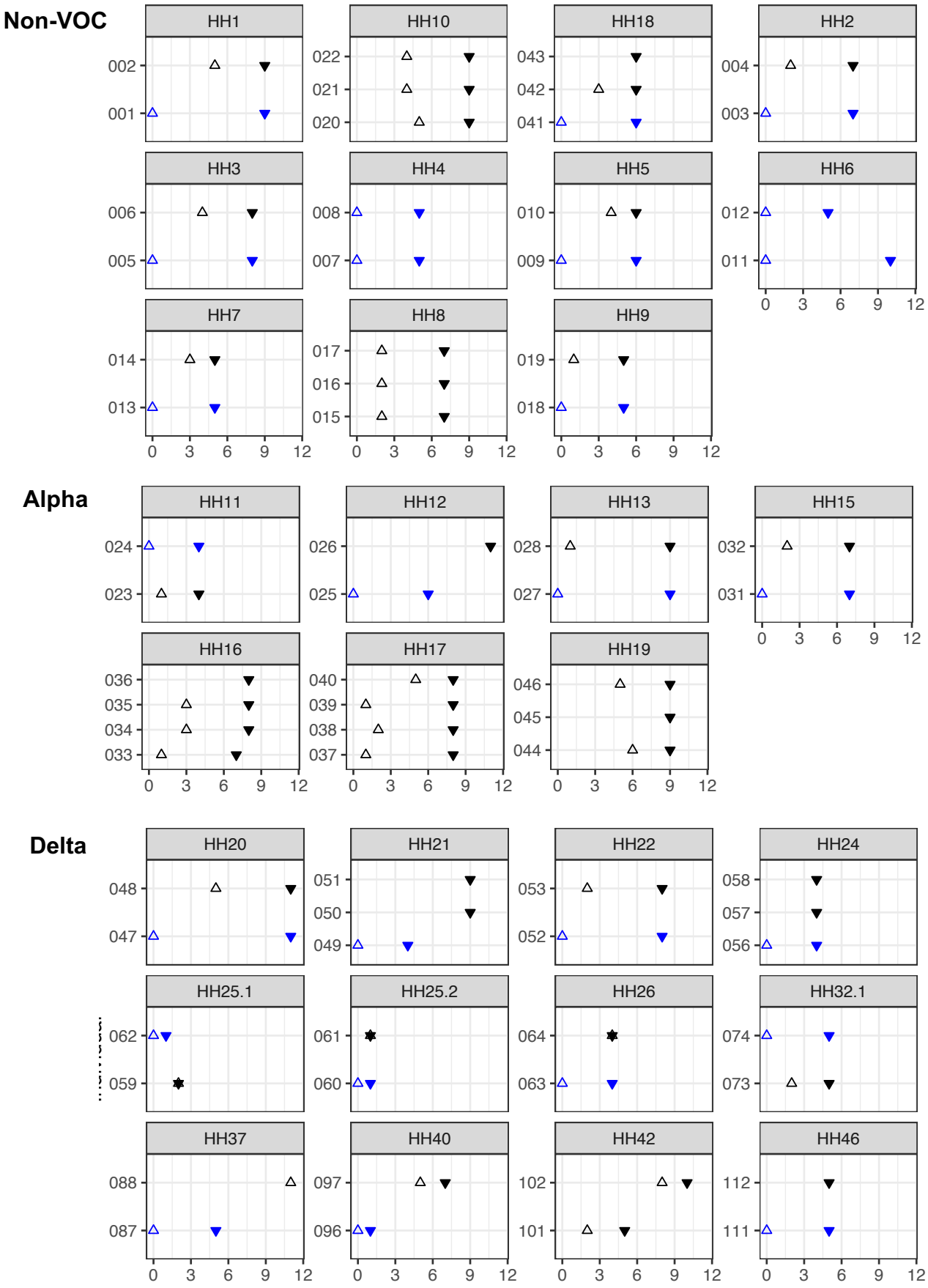

Figure S3. Timing of symptom onset and specimen collection by household. Each panel shows a household, grouped by the indicated clades. Within each household, blue symbols indicate index case(s) and black symbols indicate household contact(s). Open triangles indicate time of symptom onset and filled triangles indicate specimens that were sequenced. If there is no symptom onset, the case was considered to be asymptomatic.

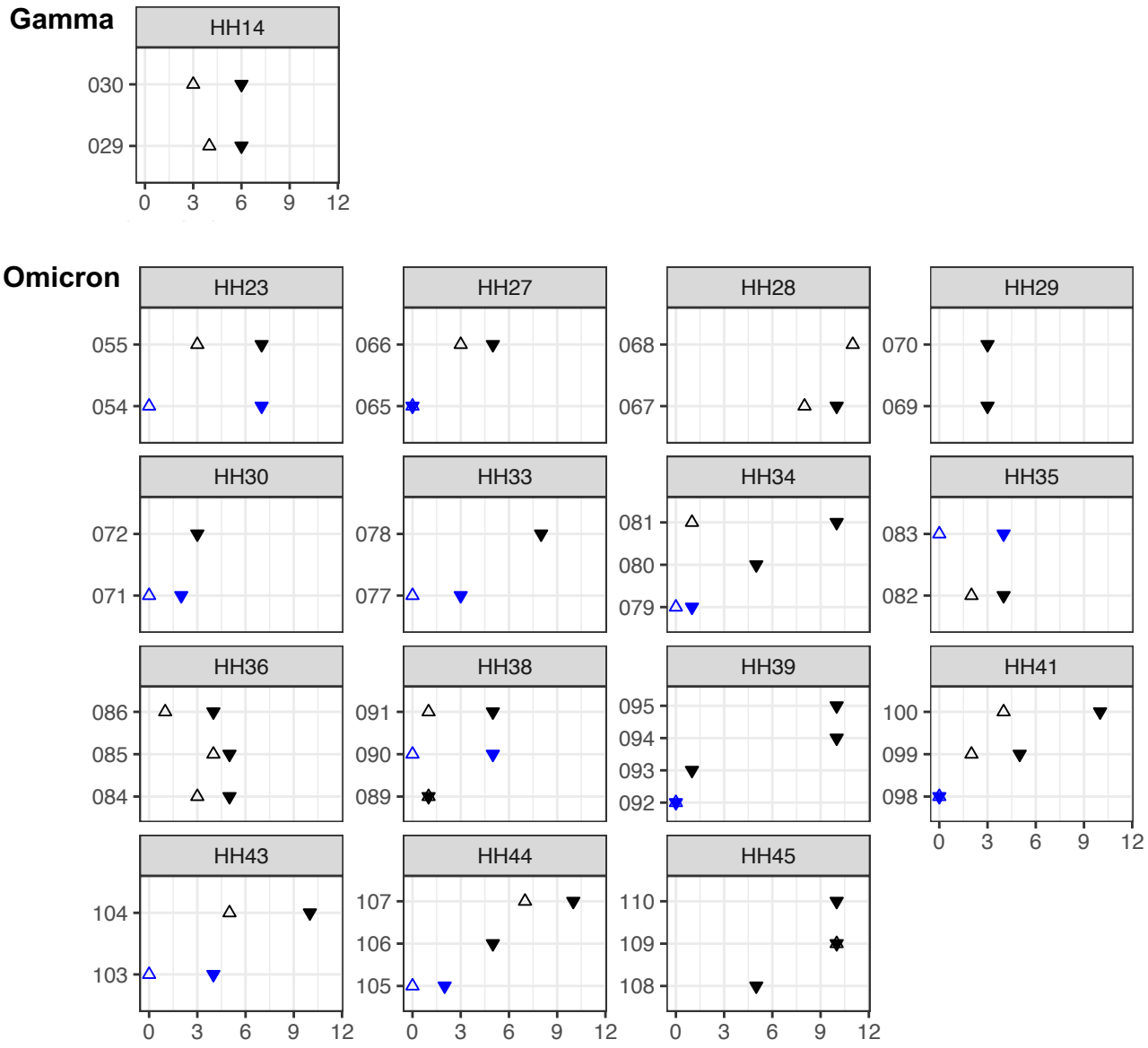

Figure S4. Timing of symptom onset and specimen collection by household. Each panel shows a household, grouped by the indicated clades. Within each household, blue symbols indicate index case(s) and black symbols indicate household contact(s). Open triangles indicate time of symptom onset and filled triangles indicate specimens that were sequenced. If there is no symptom onset, the case was considered to be asymptomatic.

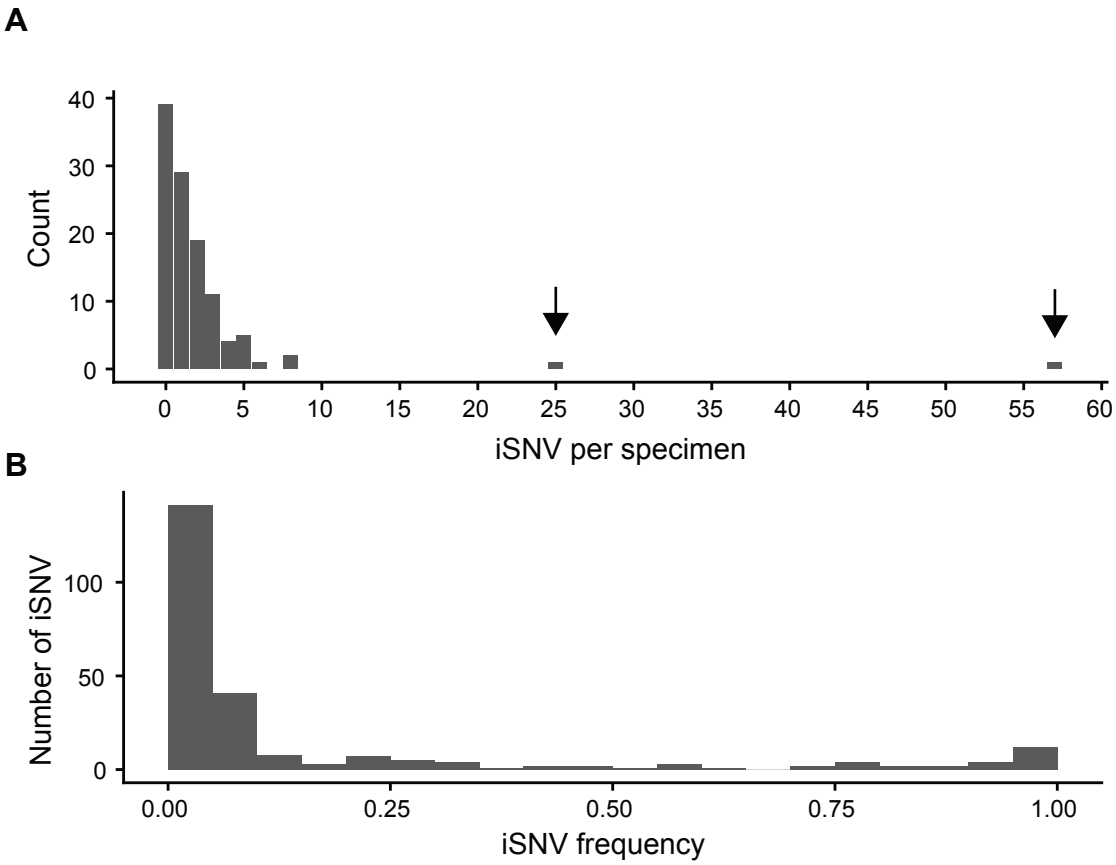

Figure S5. iSNV detected when sequencing replicates are merged. (A) The number of iSNV per specimen. Nearly still had a low number of iSNV. However, merging the reads greatly increased the number of iSNV in two individuals. These iSNV were near the 2% threshold. (B) Most iSNV were found at low frequencies. The frequency distribution shifted toward lower frequencies compared to when iSNV had to be detected in both replicates.